Electronic supplementary materials *Mendeleev Commun.*, 2026, **36**, 123–134

Primary photophysical and photochemical processes in promising light-activated anticancer complexes of platinum, ruthenium and rhodium

Evgeni M. Glebov, Valeriya A. Meshcheryakova and Alexei A. Melnikov

S1 Basics of PDT and PACT

Cancer is a disease characterized by abnormal and uncontrolled cell growth that can spread to other parts of the body.[S1] Despite advances in treatment, it remains one of the most serious and often fatal medical conditions. Chemotherapy, the primary approach to cancer treatment, uses cytotoxic drugs to kill or inhibit cancer cells. However, its effectiveness is limited by a critical drawback such as the lack of selectivity with respect to cancerous and healthy cells.[S2] As a result, high doses of these agents damage normal tissues, leading to severe side effects and a narrow therapeutic index.[S1]

Further complicating the issue, prolonged exposure to chemotherapy can induce drug resistance in tumor cells, allowing them to evade treatment and leading to disease recurrence.[S3] Even a minor resistance can significantly reduce the efficacy of the therapy, emphasizing the need for more targeted approaches. Developing selective agents that act specifically on cancer cells could minimize toxicity, overcome resistance, and ultimately improve patient outcomes.

Prodrugs offer a promising approach to cancer therapy as they are designed to selectively accumulate and activate within or near tumor tissues, thereby increasing specificity and minimizing systemic toxicity.[S4] Several widely used anticancer agents such as mitomycin C, cyclophosphamide, procarbazine, and 5-fluorouracil (5-FU) require enzymatic activation to exert their effects.[S4] However, enzymatic activation can be inefficient or unpredictable. An alternative strategy involves photoactivation, for which non-ionizing radiation (preferably red or near infrared) is used to activate a drug precisely where and when it is needed, offering enhanced control and safety.

Therapeutic usage of light-sensitive substances dates back to ancient times, particularly for the treatment of skin disorders. One of the earliest documented examples comes from ancient Egypt where extracts from herbs and tree fruits containing compounds like psoralen were applied to treat vitiligo and other pigmentation conditions (Figure S1).[S5] This historical practice laid the foundation for modern light-based therapies, demonstrating an early understanding of how light and photosensitive agents could combat disease.

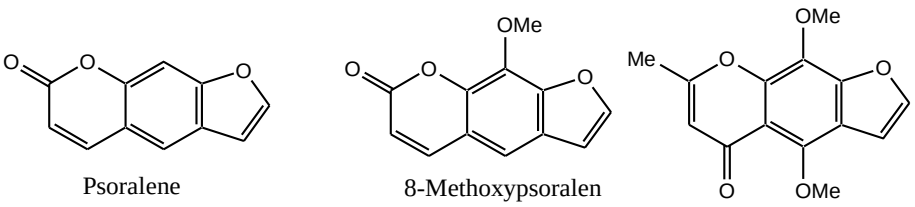

Figure S1 Light-activated compounds used from ancient times to the present day.

Nowadays phototherapy is a well-established medical treatment. It is commonly used not only for dermatological disorders such as psoriasis, eczema, vitiligo, and cutaneous T-cell lymphoma but in the treatment of neonatal jaundice, neurological conditions, and dental diseases.[S6] In dentistry, phototherapy is particularly applied in the management of periodontal disorders such as periodontitis.[S6] Phototherapy belongs to a broader class of light-based therapeutic approaches that combine electromagnetic radiation with photosensitizers. These strategies enable precise targeting of affected cells, laying the groundwork for modern treatments such as photodynamic therapy (PDT) and photoactivated chemotherapy (PACT).[S4,S7-S9]

A closer look at the mechanistic basis of the PDT will provide insight into how light-induced processes can be harnessed for selective cancer treatment. Photodynamic therapy is a minimally invasive treatment that combines electromagnetic radiation with photosensitizing agents to selectively destroy cancer cells. The photosensitizer is administered orally or intravenously and remains inactive until exposed to light of a specific wavelength. Once absorbed by target cells, the compound is activated by localized light exposure triggering photochemical reactions that generate reactive oxygen species (ROS). These ROS initiate a cascade of biochemical events, ultimately leading to the destruction of nearby cancer cells. A general overview of PDT stages is presented in Figure S2.[S4,S10-S13]

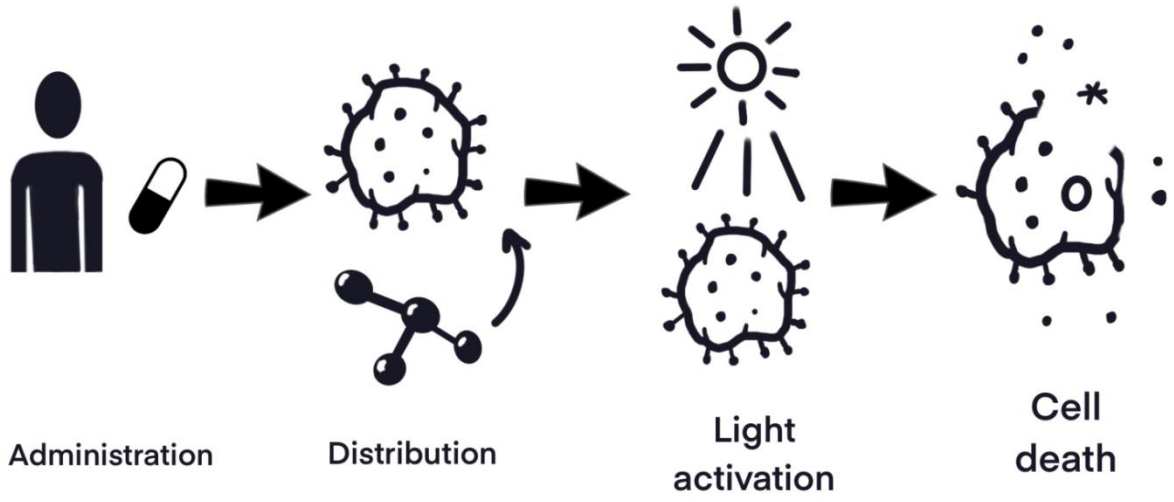

Figure S2 Schematic representation of the photodynamic therapy stages.

The key feature of all light-induced chemical transformations is the alteration of the molecule's electronic structure upon excitation to higher energy levels. Compared to thermal activation (0–150 kJ mol^{-1}), photoactivation requires significantly more energy (~ 110–550 kJ mol^{-1})[S14], which enables access to a broader and more selective range of reaction pathways.

In the simplest scenario, the excited molecule returns to its ground state by dissipating excess energy as heat or light *via* fluorescence (from a singlet excited state) or phosphorescence (from a triplet state). However, the energy of an excited photosensitizer can also be transferred to molecular oxygen (normally in a triplet ground state), generating highly reactive singlet oxygen ($^1O_2$). Alternatively, other ROSs such as hydroxyl or hydroperoxyl radicals may be formed depending on the reaction conditions and the photosensitizer structure. Also, light excitation may trigger oxygen-independent mechanisms, such as photoinduced electron transfer, which directly alters the substrate. In transition metal complexes, these processes often involve ligand substitution, isomerization, or redox transformations of the metal center. [S4,S10-S13]

Photodynamic therapy relies on distinct photophysical and photochemical processes which can be broadly categorized into three reaction types. The Jablonski diagram illustrates these processes (Figure S3). Upon light absorption, the photosensitizer is excited from its ground singlet state (S_0) to the short-lived excited singlet state (S_1). From there, it may return to the ground state *via* fluorescence or internal conversion, or undergo intersystem crossing to the longer-lived triplet state (T_1). The triplet state plays a central role in initiating photodynamic effects.

In Type I reactions, the triplet-state photosensitizer transfers an electron to molecular oxygen or another substrate generating reactive radicals. This process may be both oxygen-independent and oxygen-dependent;[S15] in the last case superoxide ($O_2^{\bullet-}$) is formed. In oxygen-

dependent Type II reactions, energy is transferred from the triplet state to molecular oxygen producing singlet oxygen ($^1O_2$) which is typically the dominant cytotoxic species in PDT applications.[S16] However, both Type I and Type II mechanisms depend on intracellular oxygen thus limiting their efficacy in hypoxic tumor environments.[S4,S17] To overcome this, a third mechanism, Type III, has been proposed involving direct oxygen-independent electron transfer from the excited photosensitizer to cellular targets.[S10]

As noted, the therapeutic efficacy of photosensitizers in PDT is closely linked to the photophysical properties of their triplet excited states which should be long-lived, high in quantum yield, and energetically suited for efficient energy or electron transfer. Ideal photosensitizers are photostable, they selectively accumulate in tumor tissues, and absorb strongly in the therapeutic window (620–850 nm), while avoiding excessive skin sensitivity from residual absorption in the 400–600 nm range.[S18]

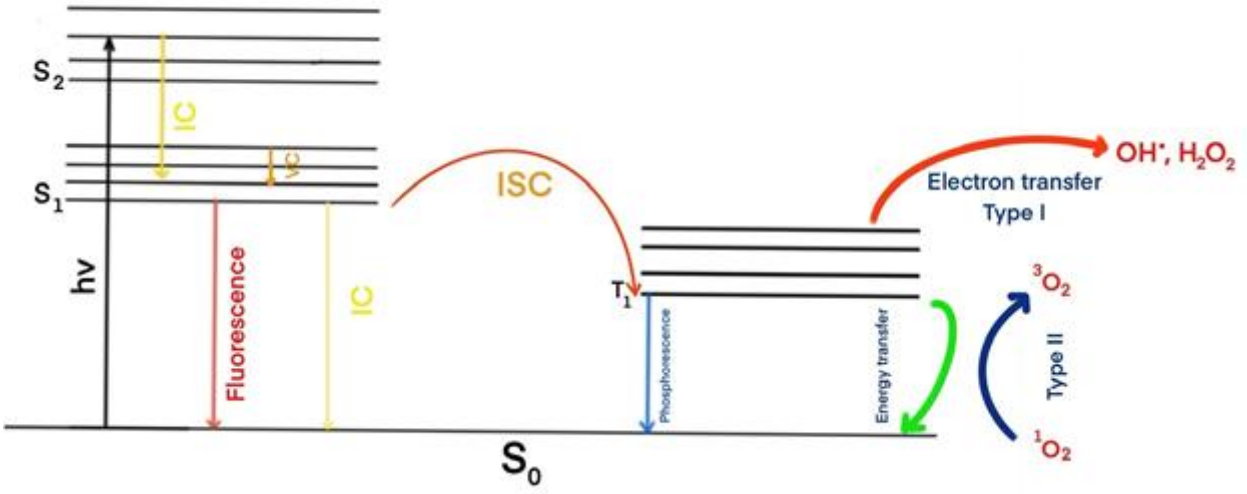

Figure S3 Jablonski diagram representing types of PDT reactions.

Several photosensitizers have already been approved for clinical use. Photofrin® (Fig. S4a) is the first-generation commercial drug, a derivative of hematoporphyrin (HpD) being a mixture containing less than 20% inactive monomers and more than 80% active dimers and oligomers. In 1986, Japanese scientists reported the results of successful treatment of lung cancer using HpD, and later Photofrin®.[S19] Photofrin® was the first photosencitizer approved in clinical practice in 1995. It was used to treat various cancers including early and late-stage lung cancer.[S13,S20] Hemoporfin (Foscan®, Figure S4, *b*) introduced in 2001 is more potent and requires significantly lower doses of both drug and light.[S13,S18] Additionally, aminolevulinic acid (ALA, Levulan®, Figure S4, *c*) and methyl aminolevulinate (Metvix®, Figure S4, *d*) are approved for topical use in the treatment of actinic keratosis. These prodrugs generate active porphyrin

photosensitizer protoporphyrin IX *in situ* upon application.[S13,S20] In review[S7] published in 2019, about 10 PDT agents were mentioned as being on the stage of clinical trials.

Russian scientists are pioneers in the application of clinical PDT in Europe. Since 1992, developments in the use of PDT in the treatment of a wide range of diseases have begun in Russia.[S21-S26] The first domestic analogue of HpD, namely Photohem, developed by the group of Prof. A.F. Mironov underwent clinical trials in 1992.[S21,S23] Alasens, a domestic drug based on aminolevulinic acid, passed clinical trials and was recommended for use in 2006.[S27] It is successfully used against bladder cancer.[S28] To date, the main trends in the development of PDT in various fields of medicine have been formulated. Researchers propose and demonstrate new technical solutions, experimental and clinical material indicating the effectiveness and safety of PDT in the treatment of tumors of various localizations.[S29]

Currently, several PDT drugs of the second generation are used in clinical practice in Russia. Photosence® (Figure S4, *e*) is a mixture of phtalocyanines.[S27,S29] Representatives of the second generation of photosensitizers also include chlorins and chlorin-like sensitizers.[S30,S32] Domestic drugs Photoditazin®, Photolon® and Photoran E6® based on the derivatives of chlorin e6[S32] (Figure S4, *f*) demonstrated high efficiency against basal cell skin carcinoma.[S31] Similar properties were reported for Radachlorin® being the sum of sodium salts of chlorin e6, chlorin p6 and purpurin 5.[S33] Photoran E6® and other chlorin e6 derivatives were successfully used for treatment of superficial bladder tumors.[S34] Photodynamic therapy with Photosence® and Photodiazin® (chlorin e6 derivative) give good results against cancer of large duodenal papilla and extrahepatic bile ducts.[S35] Chlorin e6 derivatives (Photoran E6® and Photoran E6®) are used in intraoperative PDT of sarcoma in soft tissues.[S36]

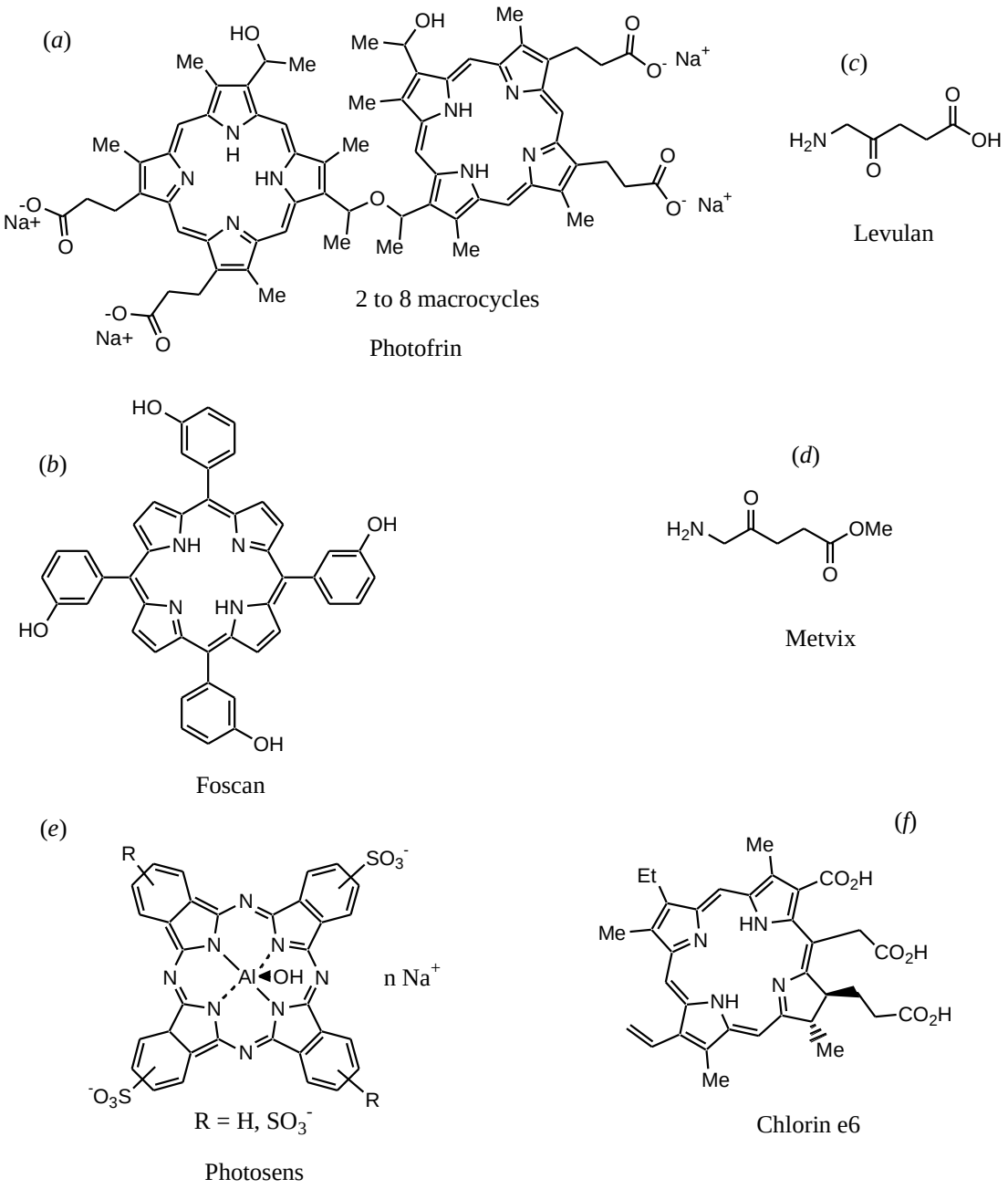

Figure S4 Clinically approved photosensitizers: (*a*) Photofrin, (*b*) Foscan, (*c*) Levulan, (*d*) Metvix, (*e*) Photosence and (*f*) Chlorin e6.

Despite evident successes, the oxygen dependency of PDT remains a major limitation. This explains the growing interest in photoactivated platinum-group metal complexes which operate through oxygen-independent mechanisms and offer new directions for overcoming current challenges in cancer phototherapy.[S4]

Photo-activated chemotherapy (PACT) has emerged as an alternative therapeutic approach based on a different principle. In PACT, a metal complex typically from the platinum group is administered in an inert form and subsequently activated by light at the tumor site. For example, Pt^{IV} complexes can undergo photoreduction to their active Pt^{II} forms upon light exposure mimicking the cytotoxic action of cisplatin.[S4] With appropriate ligand design, both Pt^{IV}

and Pt^{II} complexes can be photolabile enabling precise spatiotemporal control over drug activation. A promising application of this concept is the development of light-sensitive Pt^{IV} prodrugs that are selectively activated by laser light inside the tumor minimizing systemic toxicity and enhancing the therapeutic index.[S4] A key advantage of PACT over traditional PDT is its independence from molecular oxygen making it especially valuable for treating hypoxic tumors.[S4,S16] Beyond platinum, other platinum-group metals such as ruthenium, iridium, and rhodium are also being explored in PACT systems due to their tunable photophysical properties and versatile coordination chemistry.[S4]

The photochemical activity of coordination compounds is deeply rooted in their electronic structure, particularly the arrangement of metal d-orbitals in an octahedral ligand field. Upon absorption of light, these complexes undergo transitions to excited states which can drive therapeutic reactivity. In the octahedral geometry, crystal field splitting leads to separation of the d-orbitals into two sets: the lower-energy t_{2g} and the higher-energy e_g orbitals. The energy gap between these orbitals known as Δ_{oct} governs the electronic transitions and is influenced by the nature of the metal center and the ligands.

Coordination compounds can exhibit several types of electronic excitation. Among the most relevant for photoactivation are metal-centered (MC), ligand-centered (LC), metal-to-ligand charge transfer (MLCT), and ligand-to-metal charge transfer (LMCT) transitions. Each of these pathways leads to different forms of reactivity. For instance, MLCT transitions commonly seen in Ru^{II} and Rh^{II} complexes promote electrons from a metal orbital to a ligand-based π^* orbital generating an excited state that is often long-lived and reactive toward molecular oxygen or biomolecular substrates.[S10] Such long-lived excited states, especially triplet MLCT or IL (intraligand), are instrumental in generating singlet oxygen $^1O_2$ or other ROSs used in PDT. For example, $[Ru(bpy)_3]^{2+}$ undergoes efficient MLCT excitation and produces $^1O_2$ with high quantum yields though it lacks strong DNA binding. Modified ligands like dppz or dppn allow for both intercalation into DNA and enhanced photoactivity.[S10] In PACT, these excited states enable oxygen-independent reactivity, which is vital for hypoxic tumor environments. $Rh_2^{II,II}$-based complexes, for instance, can enter dppn-based IL excited states and photocleave DNA through guanine oxidation without requiring oxygen. These redox-active excited states offer promising routes to direct DNA damage or photoinduced ligand release, mimicking the behavior of cisplatin in the light-controlled manner.[S10]

Ultimately, the therapeutic function of a coordination compound, whether acting through PDT or PACT, depends on the photophysical properties of its excited states. By adjusting the ligand framework, chemists can finely tune absorption wavelengths, excited-state lifetimes, and

redox potentials, allowing for both controlled drug delivery and cytotoxic effects in targeted tissues.

In summary, the application of light in cancer therapy, whether through PDT or PACT, relies on the precise control of excited-state processes in organic or coordination compounds. Platinum-group metal compounds offer remarkable versatility in this regard, with their photochemical reactivity governed by the nature of the metal center, ligand environment, and type of excited state accessed. The interplay between structure, light absorption, and biological response defines their therapeutic potential. Understanding the nature and dynamics of these excited states is therefore crucial for rational design and effective application. In the following sections, we turn our attention to the experimental techniques that allow one to probe these fast and ultrafast processes, by a discussion of how these processes manifest themselves in the photophysics and photochemistry of cytotoxic platinum-group metal complexes.

S2 Fast and ultrafast experimental techniques

The available set of experimental time-resolved methods allows one to study photophysics and photochemistry in real time. An introduction to the modern fast and ultrafast techniques can be found *e.g.* in the book.[S37] The most common time-resolved methods are laser flash photolysis with time resolution of several nanoseconds and luminescent methods with time resolution from tens of picoseconds. Methods with resolution from 10 fs to 1 ns are considered as ultrafast. One of the pioneers in the application of ultrafast lasers in chemistry was the Nobel laureate Ahmed Hassan Zewail.[38] Here we give a brief description of the ultrafast spectroscopy methods. More detailed information can be found in reviews.[S39-S50]

Pump-probe (transient absorption). The most common approach is the registration of intermediate absorption in the visible and UV range (ultrafast pump-probe transient absorption (TA) spectroscopy).[S51] In Russia it is realized in The Institute of Spectroscopy RAS (Troitsk, Moscow)[S52,S53] and in The Semenov Federal Research Center for Chemical Physics (Moscow).[S55,S56] The scheme of the method is typical for any flash photolysis setup. The first pulse (‘pump’) excites the system at $t = 0$. The initial radiation source is usually a femtosecond titanium-sapphire laser with the output at a central wavelength near 800 nm. Frequency doubling and tripling provide harmonics at 400 and 267 nm, respectively, while the use of parametric amplifiers allows changing the excitation wavelength continuously. After the excitation, the system is probed by the second (‘probe’) light pulse, the delay time of which relative to the pump pulse can be varied using an optical delay line. Ultrashort probe pulses are generated using nonlinear optical methods in order to cover a broad spectral range, including shorter than 300 nm (*e.g.*, the supercontinuum generation).[S56]

Up-conversion is another popular time-resolved method that allows one to study ultrafast luminescence.[S57] After excitation of the luminescence by a laser pulse, the radiation is collected by wide-angle optics and focused onto a nonlinear crystal. The crystal mixes the luminescence with the femtosecond gate pulse (usually the fundamental output of the Ti-sapphire laser), the delay time of which with respect to the excitation pulse can be varied. The temporal evolution of the luminescence intensity can be monitored by detecting the sum-frequency ('up-converted') radiation as a function of the gate pulse delay time. In most up-conversion experiments luminescence is detected at a single wavelength. However, several schemes were developed that allow recording a broad luminescence spectrum at each delay time.[S58]

Both the pump-probe and the up-conversion experiments do not provide direct information about the nature (structure, spin, charge) of the registered excited states and intermediates. The properties of the intermediates are postulated when choosing a model of the ultrafast process; theoretical considerations (*e.g.*, quantum-chemical calculations of the absorption spectra of the supposed excited states or intermediates) are often used to support the suggested interpretation.

Ultrafast IR spectroscopy in combination with quantum-chemical calculations of vibrational frequencies of probable intermediates provides greater potential for structure determination than UV spectroscopy, regardless of the time range. The rapid development of the ultrafast IR spectroscopy began at the end of the 20th century.[S59] An additional advantage of the IR range is the possibility of direct observation of vibrational relaxation and solvent relaxation.[S60]

Ultrafast 2D spectroscopy. Advances in nonlinear optics in the last two decades have given impetus to the development of ultrafast 2D spectroscopy.[S61] The possibility of continuously changing the excitation wavelength is achieved using optical parametric amplifiers (OPA, and NOPA, non collinear optical parametric amplifier). Thus, in the setup described in work[S62] the system (Ti:Sapphire laser + NOPA) created a visible light continuum (540 – 720 nm) after which the frequency was doubled and a narrow (1.5 nm) band was allocated for excitation. As a result, excitation is possible in the range of 200 – 400 nm. The duration of the excitation pulses in the original version of the setup was 150 fs[S62] the subsequent modification made it possible to reduce the duration to 50 fs.[S63] Probing was carried out by a continuum in the range of 245 - 380 nm.

Ultrafast 2D IR spectroscopy. There exists an IR version of 2D spectroscopy using broadband IR excitation and IR probing with a continuum obtained in a Ti:Sapphire laser + NOPA system. In the setup described in,[S64] an emission band with a maximum at 1650 cm^{-1}, a width of 130 cm^{-1} and duration of 150 fs was used. When structural groups of a molecule

interact, off-diagonal cross peaks similar to cross peaks in 2D NMR spectroscopy arise in the 2D IR spectrum. If 2D NMR spectroscopy is used to study the spatial structure of complex molecules, 2D IR spectroscopy can be used to study ultrafast movements of structural groups.[S64]

Ultrafast photoelectron spectroscopy (PES) is based on measuring the energy spectra of electrons emitted from a sample during photoelectron emission. The method allows one to determine the absolute values of the binding energy (work function) of states. Thus, one can directly determine the valence of a metal cation in a complex. For a long time, the application of PES to liquid samples was a problem due to the incompatibility of the volatility of the sample and the vacuum required for the operation of the device. The problem was solved at the end of the 20th century in the works of Faubel and Winter who created a microjet technology for injecting a liquid sample into vacuum.[S65] At the beginning of the current century, Faubel and Abel with co-workers created time-resolved (ultrafast) PES.[S66]

The ultrafast PES requires a bright ultrafast source of UV or X-ray radiation. Many modern table top setups are based on the effect of high harmonic generation (HHG).[S67] When an intense laser pulse is focused in gas (usually noble gases at reduced pressure), strong nonlinear interactions lead to the generation of high order odd harmonics of the original optical pulse. This usually occurs at intensities of the order of 10^{14} W cm^{-2} or higher. Starting with the radiation of a Ti:Sapphire laser (800 nm), it is possible to obtain quanta with energies up to the vacuum ultraviolet and soft X-ray range.[S68] Thus, in the experimental setup of the Lausanne Ultrafast Research Center (Chergui *et al.*[S69]), vacuum ultraviolet with an energy of 39 eV (the 25th harmonic of the Ti:Sapphire laser) is generated. This radiation is used for probing in the pump-probe scheme.

Ultrafast X-ray spectroscopy. The described ultrafast methods do not provide direct information on the change in the structure of excited molecules. Such information can be obtained by probing in the X-ray range,[S70-S72] which requires a source of ultrashort X-ray pulses. All such sources can be divided into two classes, namely, laboratory setups and large machines. Laboratory ('table top') setups include the already mentioned HHG[S67,S68] and laser-plasma radiation sources[S70] that can generate X-ray pulses with a duration of 100 fs. Such setups are limited in energy to the range from vacuum ultraviolet (10 - 100 eV) to soft X-rays (100 eV - 6 keV). Large machines include particle accelerators (synchrotrons). They generate X-ray pulses with a duration of ~ 100 ps, but pulses as short as ~ 100 fs can be obtained using the so-called femtosecond slicing methods.[S71] Another class of large machines are X-ray free-electron lasers which can generate pulses with a duration of several femtoseconds.

Thus, modern experimental technology provides multiple opportunities for studying various aspects of ultrafast photoprocesses. However, for the case of light-activated anti-cancer metal complexes the applications of these methods are scarce.

S3 Selected experimental data on complexes promising in PACT

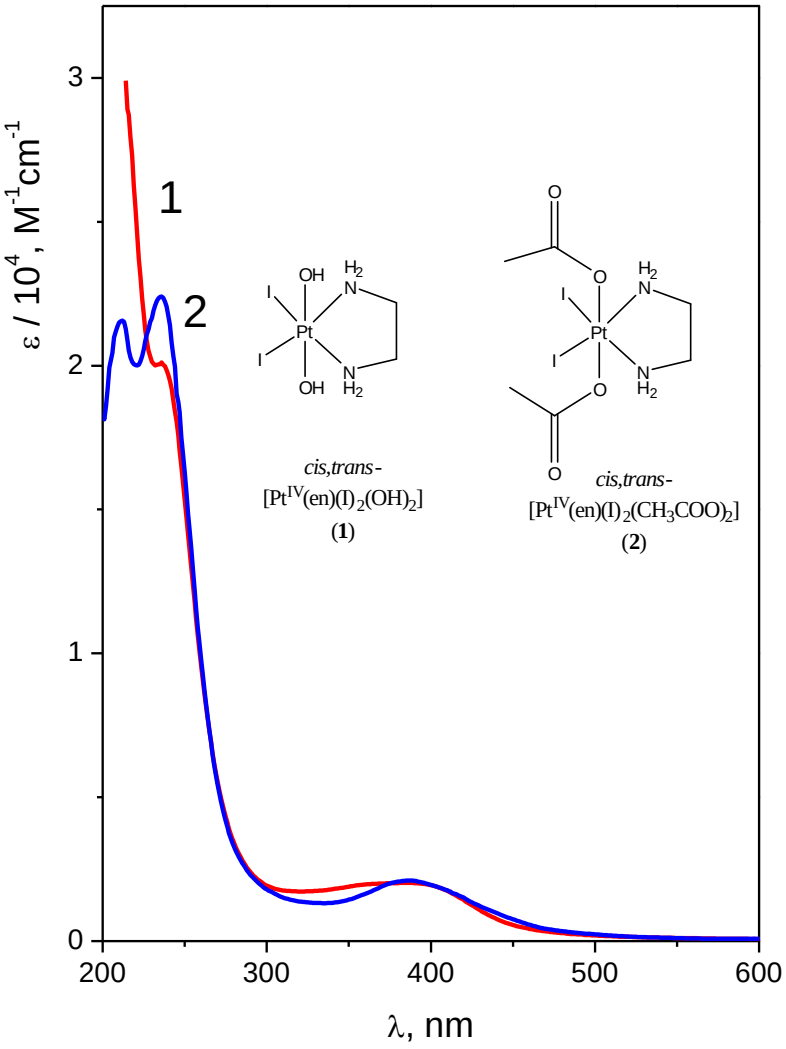

Figure S5. Electronic absorption spectra of complexes *cis,trans*-[Pt^{IV}(en)$(I)_2(OH)_2$] (**1**) and *cis,trans*-[Pt^{IV}(en)$(I)_2(OAc)_2$] (**2**) in aqueous solutions.

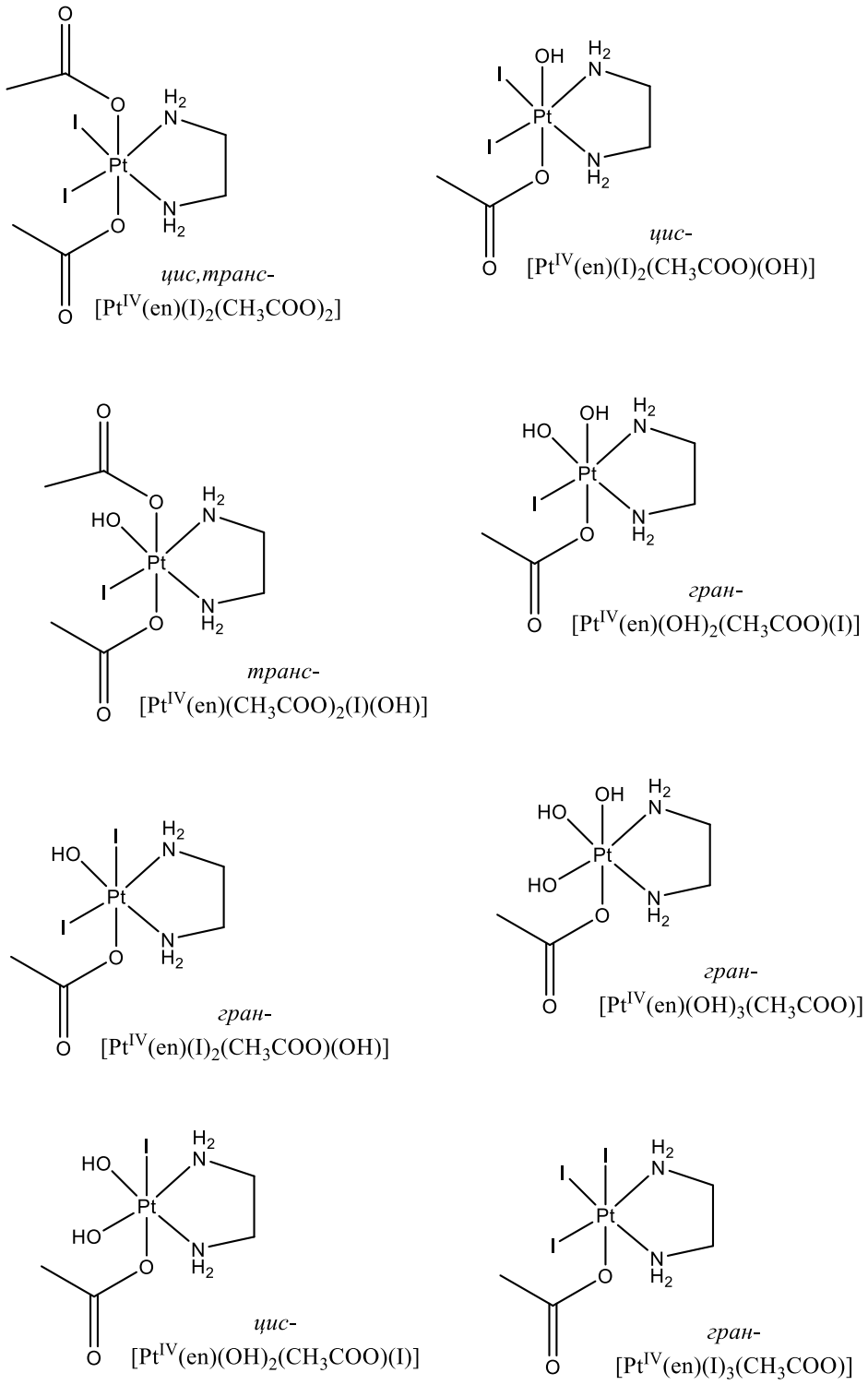

Figure S6. Products of complex **2** (*cis*,*trans*-[$Pt^{IV}(en)I_2(OAc)_2$]) photolysis containing an acetate group.

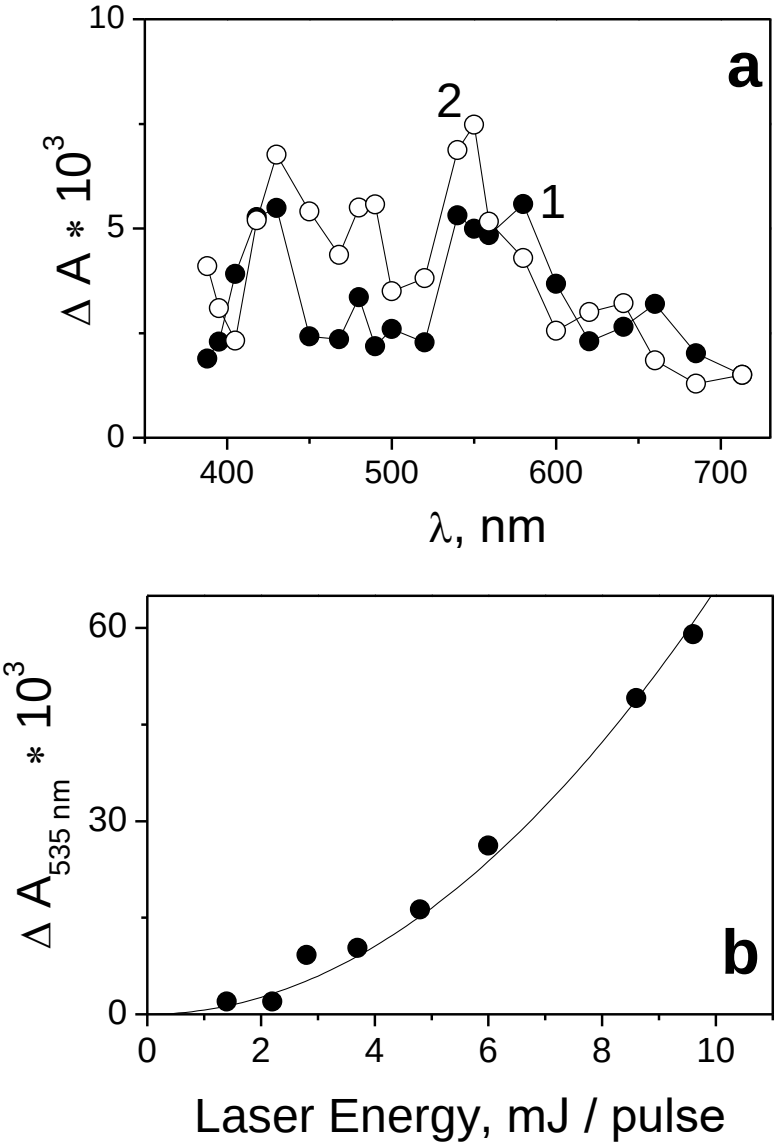

Figure S7. Results of laser flash photolysis experiments (λ_{pump} = 355 nm) with complex **2** (*cis*,*trans*-[Pt^{IV}(en)I_2(OAc)$_2$]) (2.9×10^{-4} M, pH 7.4, 1 cm cell). **a** – spectra of successive Pt^{III} intermediates (laser energy ca. 6 mJ/pulse). **b** – dependence of maximal absorption at 530 nm vs/ laser pulse energy. Adapted from ref.[S73] with permission from Springer Nature.

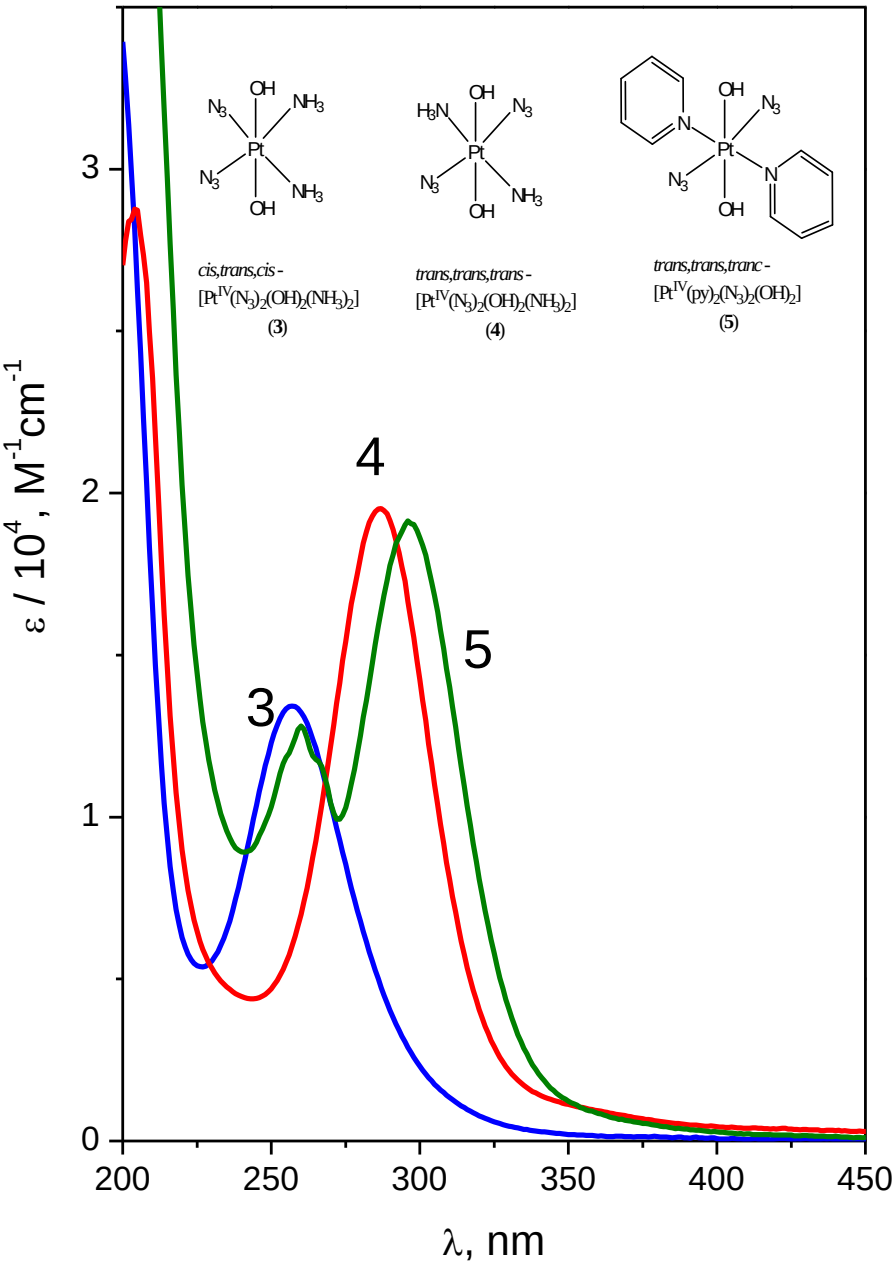

Figure S8. Electronic absorption spectra of complexes *cis*,*trans*,*cis*-[$Pt^{IV}(N_3)_2(OH)_2(NH_3)_2$] (**3**), *trans*,*trans*,*trans*-[$Pt^{IV}(N_3)_2(OH)_2(NH_3)_2$] (**4**) and *trans*,*trans*,*trans*-[$Pt^{IV}(py)(N_3)_2(OH)_2$] (**5**) in aqueous solutions.

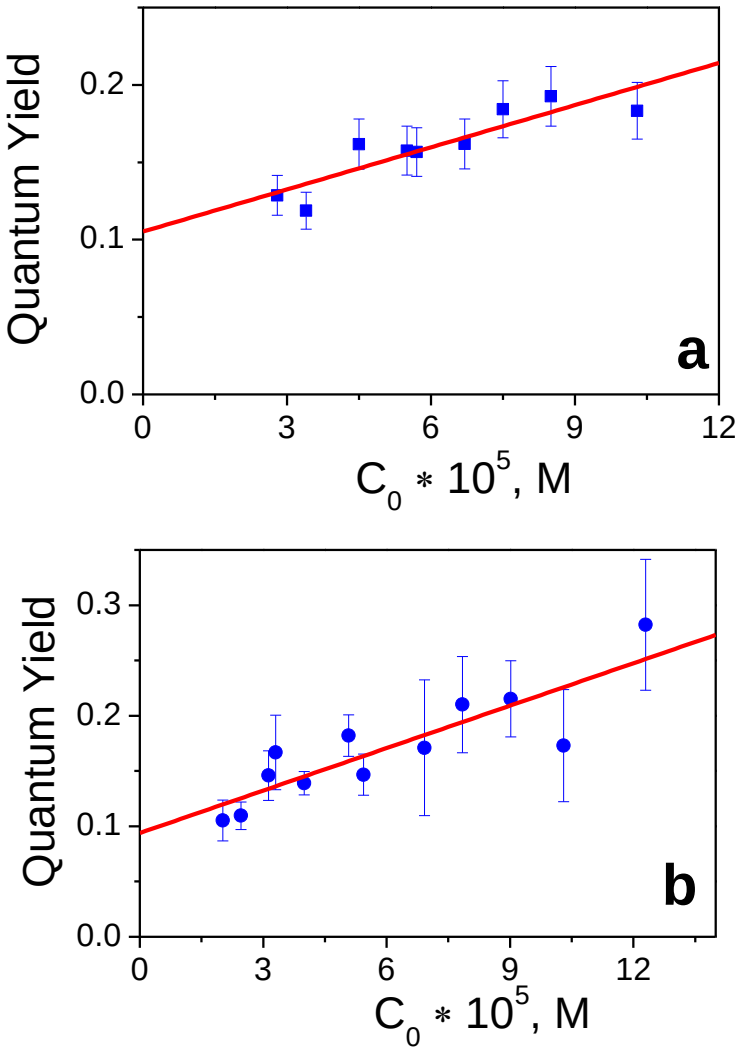

Figure S9. Dependencies of quantum yields of **3** (panel **a**) and **4** (panel **b**) photoaquation (λ_{pump} = 282 nm, photon flux density 8×10^{15} photons·cm^{-3} s^{-1}) vs. concentration of initial complexes. Structures of complexes are shown in Figure S8. Reproduced from ref.[S74] with permission from RSC Publishing.

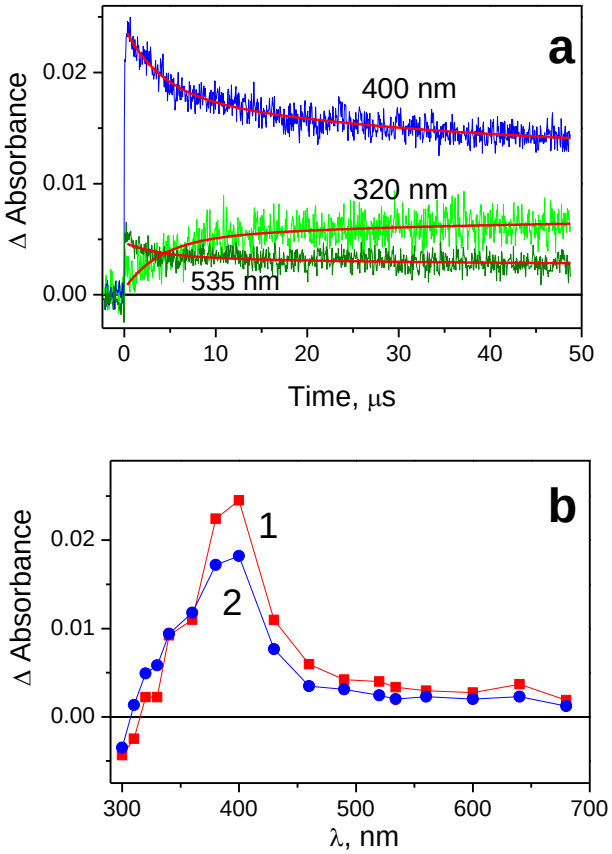

Figure S10. Results of laser flash photolysis (266 nm) experiment with complex **3** (Figure S8) in water (pH 7.4; initial concentration 5.8×10^{-5} M; 1 cm cell; air saturated solutions). **a** – characteristic kinetic curves and fits (red lines). Global fit function (4) with parameters: τ_1 = 3.9 μs, τ_2 = 32 μs. **b** – intermediate absorption spectra; curves 1 and 2 correspond to time delays 0.4 and 10 μs after the laser pulse. Reproduced from ref.[S74] with permission from RSC Publishing.

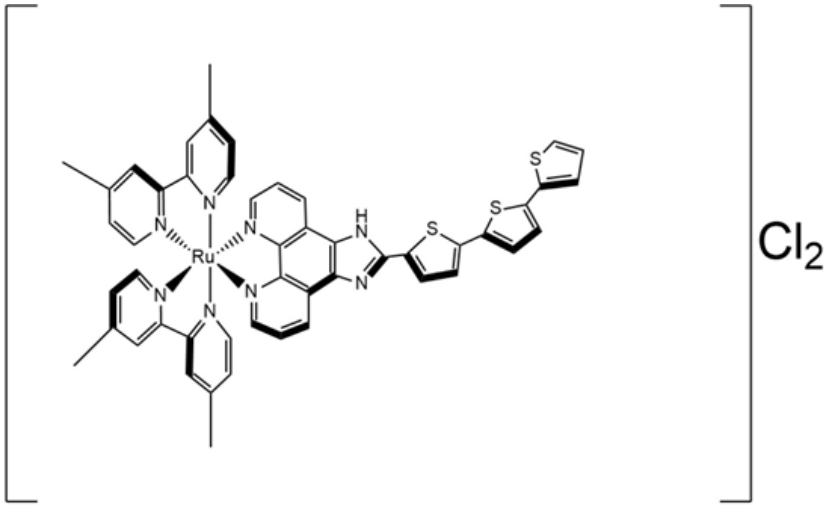

Figure S11. TLD1433, which is the first ruthenium complex approved for clinical trials as a photosensitizer for PDT.

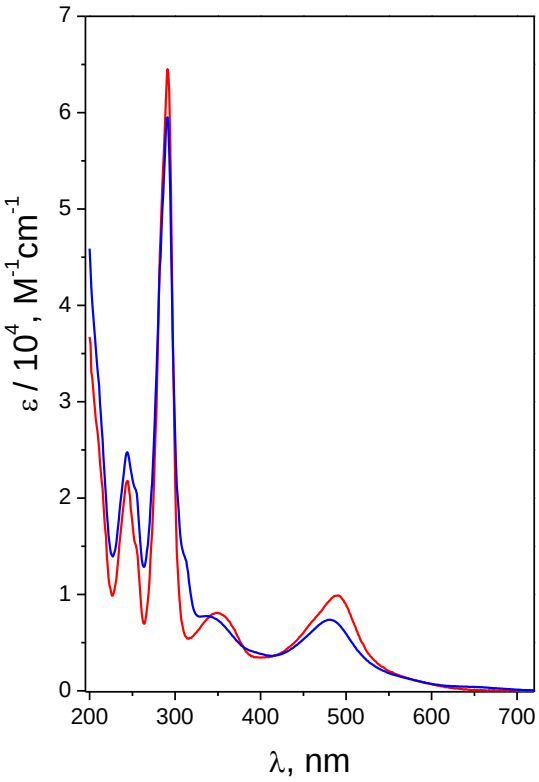

Figure S12. UV-Vis absorption spectra of *cis*-$[Ru(bpy)_2(NH_3)_2]^{2+}$ (complex **6**, red curve) and *cis*-$[Ru(bpy)_2(H_2O)(OH)]^{+}$ (complex **7,** blue curve) in aqueous solutions.

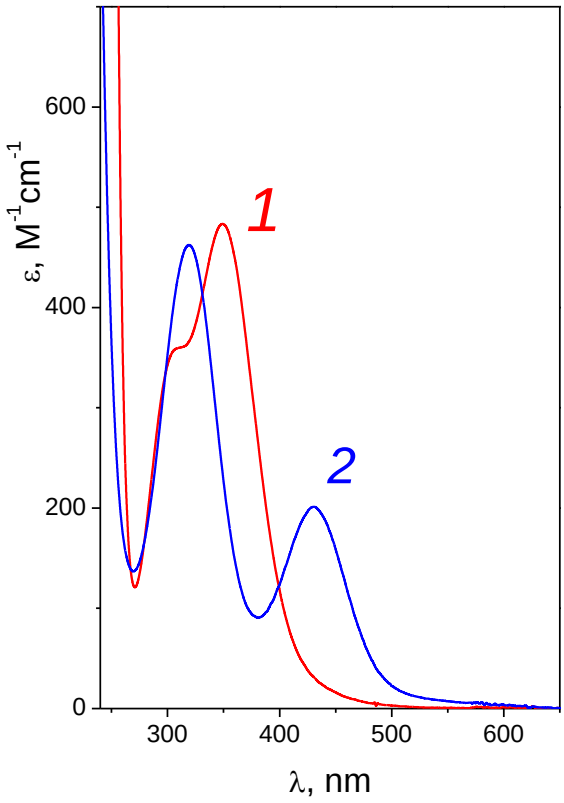

Figure S13. Electronic absorption spectra of *cis*,*fac*-$[RuCl_2(DMSO)_3(H_2O)]$ (**8a**) (curve *1*) and *trans*,*cis*,*cis*-$[RuCl_2(DMSO)_2(H_2O)_2]$ (**9a**) (curve *2*).

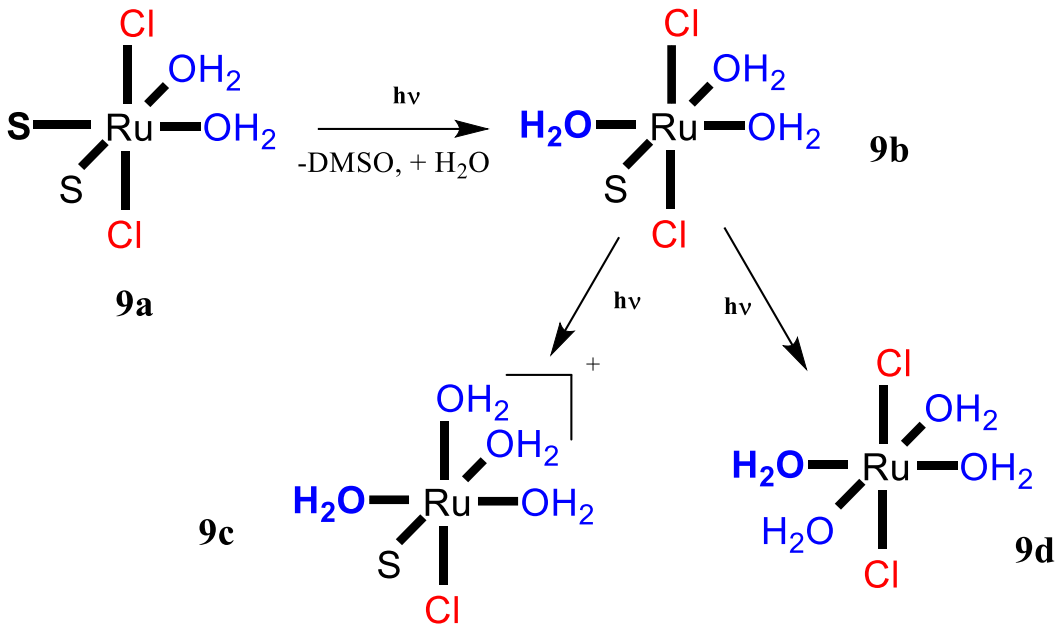

Figure S14. Photochemical reactions caused by irradiation of *trans,cis,cis*-$[RuCl_2(DMSO)_2(H_2O)_2]$ (**9a**) (430 nm) of complex in argon-saturated aqueous solutions.

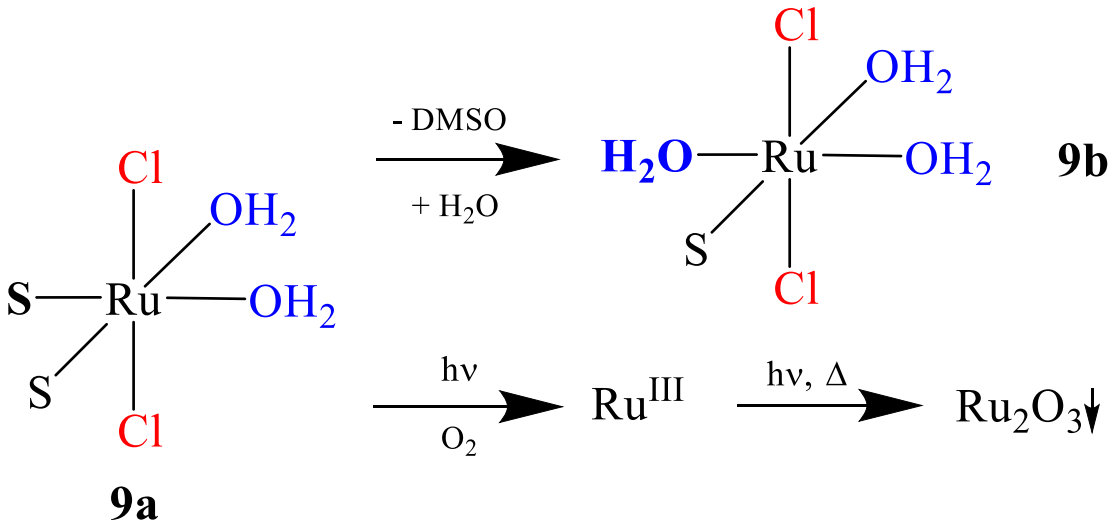

Figure S15. Scheme of photochemical reactions caused by photolysis of *trans,cis,cis*-$[RuCl_2(DMSO)_2(H_2O)_2]$ (**9a**) in aerobic aqueous solutions.

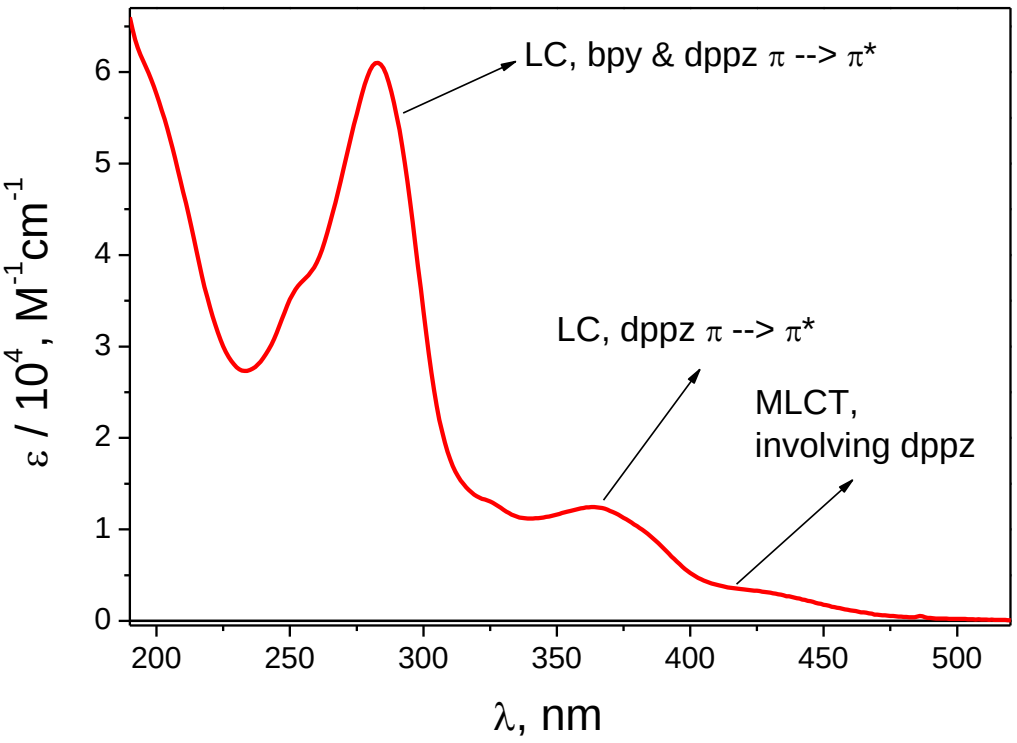

Figure S16. Electronic absorption spectrum of $[Rh_2(\mu\text{-}OAc)_2(bpy)(dppz)]^{2+}$ (complex **10**) in aqueous solutions. The main electron transitions are marked.

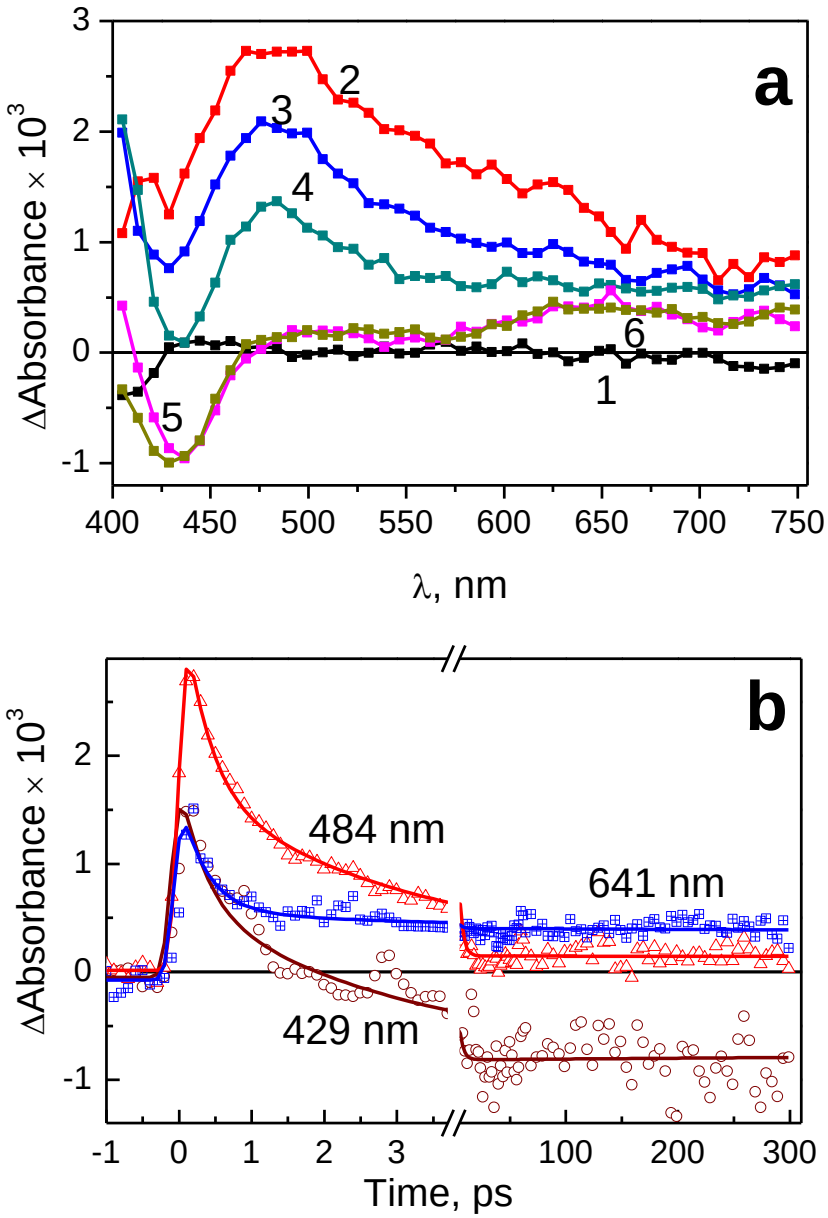

Figure S17. Results of the experiment on the ultrafast pump-probe spectroscopy (320 nm) of $[Rh_2(\mu\text{-}OAc)_2(bpy)(dppz)]^{2+}$ (complex **10**) in aqueous solutions (7.6×10^{-4} M, 1 mm cell). **a** - examples of intermediate absorption spectra. Curves 1-6 correspond to delays between pump and probe pulses equal to -1; 0.15; 0.5; 1.2; 50; 289 ps accordingly. **b** – examples of the kinetic curves, experimental points and results of a 3-exponential fit with the characteristic lifetimes 350 fs, 3.2 ps and infinity. Reproduced from ref.[S75] with permission from Springer Nature.

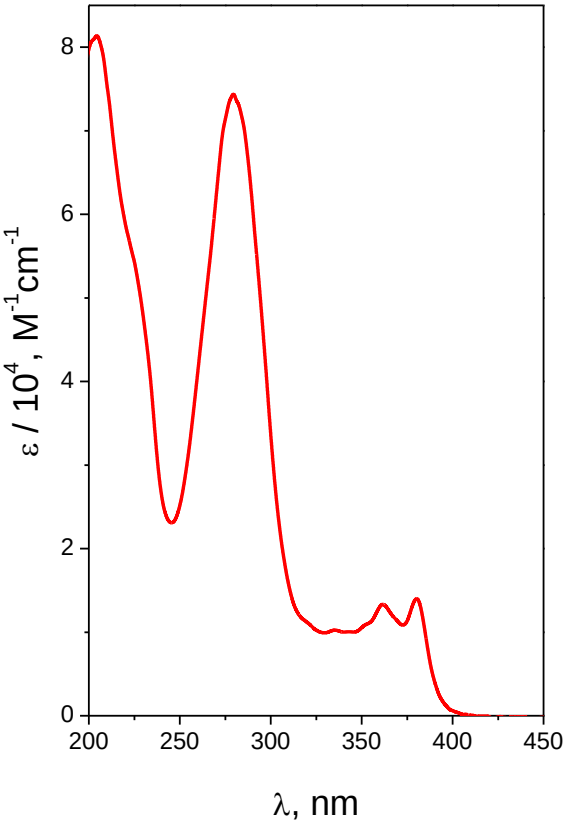

Figure S18. Electronic absorption spectrum of *cis*-[Rh(dppz)(phen)Cl_2]Cl (complex **11**) in aqueous solution.

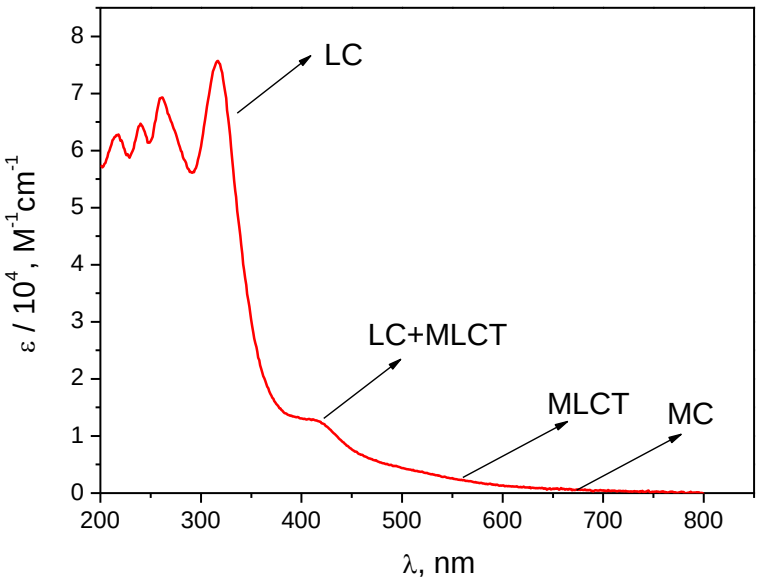

Figure S19. Electronic absorption spectrum of $Rh_2(\mu\text{-}OAc)_2(dppn)_2$ (complex **16**) in aqueous solution. The main electron transitions are marked.

References

S1 U. Anand, A. Dey, A. K. Singh Chandel, R. Sanyal, A. Mishra, D. K. Pandey, V. De Falco, A. Upadhyay, R. Kandimalla, A. Chaudhary, J. Kaur Dhanjal, S. Dewanjee, J. Vallamkondu and J. M. Pérez de la Lastra, *Genes Dis*., 2023, **10**, 1367; https://doi.org/10.1016/j.gendis.2022.02.007.

S2 F. Torino, A. Barnabei, R. Paragliola, R. Baldelli, M. Appetecchia and S. M. Corsello, *Thyroid*, 2013, **23**, 1345; https://doi.org/10.1089/thy.2013.0241.

S3 V. T. DeVita, Jr. and E. Chu, *Cancer Res*., 2008, **68**, 8643; https://doi.org/10.1158/0008-5472.CAN-07-6611.

S4 P. J. Bednarski, F. S. Mackay and P. J. Sadler, *Anti-Cancer Agents Med. Chem*., 2007, **7**, 75; https://doi.org/10.2174/187152007779314053.

S5 F. Conforti, M. Marrelli, F. Menichini, M. Bonesi, G. Statti, E. Provenzano and F. Menichini, *Curr. Drug Ther*., 2009, **4**, 38; https://doi.org/10.2174/157488509787081886.

S6 L. Ding, Z. Gu, H. Chen, P. Wang, Y. Song, X. Zhang, M. Li, J. Chen, H. Han, J. Cheng and Z. Tong, *Ageing Res. Rev*., 2024, **94**, 102183; https://doi.org/10.1016/j.arr.2024.102183.

S7 S. Monro, K. L. Colón, H. Yin, J. Roque III, P. Konda, S. Gujar, R. P. Thummel, L. Lilge, C. G. Cameron and S. A. McFarland, *Chem. Rev*., 2019, **119**, 797; https://doi.org/10.1021/acs.chemrev.8b00211.

S8 V. J. Gurruchaga-Pereda, A. Martínez, A. Terenzi and L. Salassa, *Inorg. Chim. Acta*, 2019, **495**, 118981; https://doi.org/10.1016/j.ica.2019.118981.

S9 N. J. Farrer, L. Salassa and P. J. Sadler, *Dalton Trans*., 2009, **48**, 10690; https://doi.org/10.1039/B917753A.

S10 J. D. Knoll and C. Turro, *Coord. Chem. Rev*., 2015, **282–283**, 110; https://doi.org/10.1016/j.ccr.2014.05.018.

S11 L. K. McKenzie, H. E. Bryant and J. A. Weinstein, *Coord. Chem. Rev*., 2019, **379**, 2; https://doi.org/10.1016/j.ccr.2018.03.020.

S12. L. E. Joyce, J. D. Aguirre, A. M. Angeles-Boza, A. Chouai, P. K.-L. Fu, K. R. Dunbar and C. Turro, *Inorg. Chem*., 2010, **49**, 5371; https://doi.org/10.1021/ic100588d.

S13 Á. Juarranz, P. Jaén, F. Sanz-Rodríguez, J. Cuevas and S. González, *Clin. Transl. Oncol.*, 2008, **10**, 148; https://doi.org/10.1007/s12094-008-0172-2.

S14 J. Sýkora and J. Šhima, *Coord. Chem. Rev*., 1990, **107**, 1; https://doi.org/10.1016/0010-8545(90)80055-X.

S15 P. Agostinis, K. Berg, K. A. Cengel, T. H. Foster, A. W. Girotti, S. O. Gollnick, S. M. Hahn, M. R. Hamblin, A. Juzeniene, D. Kessel, M. Korbelik, J. Moan, P. Mroz, D. Nowis, J. Piette, B. C. Wilson and J. Golab, *Ca-Cancer J. Clin*., 2011, **61**, 250; https://doi.org/10.3322/caac.20114.

S16 K. Szaciłowski, W. Macyk, A. Drzewiecka-Matuszek, M. Brindell and G. Stochel, *Chem. Rev*., 2005, **105**, 2647; https://doi.org/10.1021/cr030707e.

S17 S. Medici, M. Peana, V. M. Nurchi, J. A. Lachowicz, G. Crisponi and M. A. Zoroddu, *Coord. Chem. Rev*., 2015, **284**, 329; https://doi.org/10.1016/j.ccr.2014.08.002.

S18 E. S. Nyman and P. H. Hynninen, *J. Photochem. Photobiol., B*, 2004, **73**, 1; https://doi.org/10.1016/j.jphotobiol.2003.10.002.

S19 H. Kato, C. Konaka, N. Kawate, H. Shinohara, K. Kinoshita, M. Noguchi, S. Ootomo and Y. Hayata, *Chest*, 1986, **90**, 768; https://doi.org/10.1378/chest.90.5.768.

S20 R. Ackroyd, C. Kelty, N. Brown and M. Reed, *Photochem. Photobiol*., 2001, **74**, 656; https://doi.org/10.1562/0031-8655(2001)0740656THOPAP2.0.CO2.

S21 S. M. Bataev, K. S. Tsilenko, A. N. Osipov, A. V. Reshetnikov, A. S. Bataev and S. P. Sosnova, *Russ. J. Pediatr. Surg. Anaesth. Intensive Care*, 2022, **12**, 461 (in Russian); https://doi.org/10.17816/psaic936.
S22 M. A. Kaplan and Yu. S. Romanko, *Fizioterapiya, Bal'neologiya i Reabilitatsiya* (*Russian Journal of Physiotherapy, Balneology and Rehabilitation*), 2004, no. 1, 43 (in Russian); https://elibrary.ru/item.asp?id=17112658.
S23 E. F. Stranadko, *Fotodinamicheskaya Trapiya i Fotodiagnostika* (*Photodynamic Therapy and Photodyagnosis*), 2015, **4**(1), 3 (in Russian); https://doi.org/10.24931/2413-9432-2015-4-1-3-10.
S24 V. V. Kuznetsov, *Issledovaniya i Praktika v Medizine* (*Research and Practical Medicine Journal*), 2015, **2**(4), 98 (in Russian); https://doi.org/10.17709/2409-2231-2015-2-4-98-105.
S25 E. V. Filonenko and V. I. Ivanova-Radkevich, *Biomedical Photonics*, 2024, **13**(4), 33; https://doi.org/10.24931/2413-9432-2024-13-4-33-39.
S26. E. V. Nadkernichnaya, M. V. Ermoschenkova, V. E. Semin, S. A. Parts, V. N. Galkin and I. V. Reshetov, *Biomedical Photonics*, 2025, **14**(2), 27; https://doi.org/10.24931/2413-9432-2025-14-2-27-30.
S27 V. V. Sokolov, V. I. Chissov, E. V. Filonenko, R. I. Yakubovskaya, E. A. Lukyanets, G. N. Vorozhtsov and S. G. Kuzmin, *Ross. Bioterapevticheskii Zh.* (*Russ. J. Biother*.), 2006, **5**(1), 32 (in Russian); https://elibrary.ru/download/elibrary_13067440_64022195.pdf.
S28 E. V. Filonenko, A. D. Kaprin, B. Ya. Alekseev, O. I. Apolikhin, E. K. Slovokhodov, V. I. Ivanova-Radkevich and A. N. Urlova, *Photodiagn. Photodyn. Ther.*, 2016, **16,** 106; https://doi.org/10.1016/j.pdpdt.2016.09.009.
S29 E. V. Filonenko, *Fotodinamicheskaya Trapiya i Fotodiagnostika* (*Photodynamic therapy and photodyagnosis*), 2014, **3**(1), 3 (in Russian). https://elibrary.ru/item.asp?id=21853965.
S30 Z. S. Smirnova, I. Yu. Kubasova, O. A. Makarova, A. P. Polozkova, O. L. Orlova, N. A. Oborotova, G. A. Meerovich, G. K. Gerasimova, E. A. Lukyanetz, S. G. Kuz'min and G. N. Vorozhtsov, *Ross. Bioterapevticheskii Zh.* (*Russ. J. Biother*.), 2003, **2**(4), 40 (in Russian); https://elibrary.ru/item.asp?id=9459328.
S31 V. N. Kapinus, M. A. Kaplan, E. V. Yaroslavtseva-Isayeva, I. S. Spichenkova and S. A. Ivanov, *Issledovaniya i Praktika v Medizine* (*Research and Practical Medicine Journal*), 2021, **8**(4), 33 (in Russian); https://doi.org/10.17709/2410-1893-2021-8-4-3.
S32 A. Huk, M. Sadik-Ali, S. A. Sankaranaraynan, V. R. Shinde and A. K. Rengan, *ACS Appl. Bio Mater.*, 2023, **6**, 349; https://doi.org/10.1021/acsabm.2c00891.
S33 V. N. Volgin, E. F. Stranadko, M. V. Sadovskaya and M. V. Ryabov, *Ross. Bioterapevticheskii Zh.* (*Russ. J. Biother*.), 2009, **8**(2), 31 (in Russian); https://elibrary.ru/download/elibrary_12975689_99468209.pdf
S34 A. V. Kustov, N. L. Smirnova, O. A. Privalov, T. M. Moryganova, A. I. Strelnikov, P. K. Morshnev, O. I. Koifman, A. V. Lyubimtsev, T. V. Kustova and D. B. Berezin, *J. Clin. Med*., 2022, **11**, 233; https://doi.org/10.3390/jcm11010233.
S35 E. F. Stranadko, A. V. Baranov, V. A. Duvansky, A. I. Lobakov, V. A. Morokhotov and M. V. Riabov, *Biomedical Photonics*, 2020, **9**(2), 18; https://doi.org/10.24931/2413-9432-2020-9-2-18-28.
S36 E. V. Yaroslavtseva-Isaeva, A. L. Zubarev, V. N. Kapinus, A. A. Kurilchik, V. E. Ivanov and A. L. Starodubtsev, *Lazernaya Medizina* (*Laser Medicine*), 2022, **26**(3-4), 9 (in Russian); https://doi.org/10.37895/2071-8004-2022-26-3-4-9-15.

S37 N. V. Tkachenko. *Optical Spectroscopy: Methods and Instrumentations*, Elsevier, 2006; https://doi.org/10.1016/B978-0-444-52126-2.50049-6.
S38 A. H. Zewail, *Femtochemistry: Ultrafast Dynamics of the Chemical Bond,* World Scientific, *Vol. I,* 1994; https://doi.org/10.1142/2331.
S39 A. Vlček, Jr., *Coord. Chem. Rev*., 2000, **200-202**, 933; https://doi.org/10.1016/S0010-8545(00)00308-8.
S40 J. K. McCusker, *Acc. Chem. Res*., 2003, **36**, 876; https://doi.org/10.1021/ja00307a054.
S41 L. S. Forster, *Coord. Chem. Rev.*, 2006, **250**, 2023; https://doi.org/10.1016/j.ccr.2006.01.023.
S42 E. A. Juban, A. L. Smeigh, J. E. Monat and J. K. McCusker, *Coord. Chem. Rev.*, 2006, **250**, 1783; https://doi.org/10.1016/j.ccr.2006.02.010.
S43 S. Archer and J. A. Weinstein, *Coord. Chem. Rev.*, 2012, **256**, 2530; https://doi.org/10.1016/j.ccr.2012.07.010.
S44 J. P. Lomont, S. C. Nguyen and C. B. Harris, *Acc. Chem. Res*., 2014, **47**, 1634; https://doi.org/10.1021/ja00307a054.
S45 M. Chergui, *Dalton Trans*., 2012, **41**, 13022; https://doi.org/10.1039/C2DT30764B.
S46 M. Chergui, *Acc. Chem. Res*., 2015, **48**, 801; https://doi.org/10.1021/ar500358q.
S47 M. Chergui and E. Colet, *Chem. Rev*., 2017, **117**, 11025; https://doi.org/10.1021/acs.chemrev.6b00831.
S48 M. Chergui, *Coord. Chem. Rev*., 2018, **372**, 52; https://doi.org/10.1016/j.ccr.2018.05.021.
S49 M. Chergui, *J. Chem. Phys*., 2019, **150**, 070901; https://doi.org/10.1063/1.5082644.
S50 E. M. Glebov, *Russ. Chem. Bull*., 2022, **71**, 858; https://doi.org/10.1007/s11172-022-3486-2.
S51 N. H. Damrauer, G. Cerullo, A. Yeh, T. R. Boussie, C. V. Shank and J. K. McCusker, *Science*, 1997, **275**, 54; https://doi.org/10.1126/science.275.5296.54.
S52 S. V. Chekalin, *Phys.-Usp.*, 2006, **49**, 634; https://doi.org/10.1070/PU2006v049n06ABEH006044.
S53 E. M. Glebov, I. P. Pozdnyakov, V. P. Chernetsov, V. P. Grivin, A. B. Venediktov, A. A. Melnikov, S. V. Chekalin and V. F. Plyusnin, *Russ. Chem. Bull*., 2017, **66**, 418; https://doi.org/10.1007/s11172-017-1749-0.
S54 I. V. Shelaev, F. E. Gostev, M. D. Mamedov, O. M. Sarkisov, V. A. Nadtochenko, V. A. Shuvalov and A. Y. Semenov, *Biochim. Biophys. Acta Bioenerg.*, 2010, **1797**, 1410; https://doi.org/10.1016/j.bbabio.2010.02.026.
S55 D. A. Cherepanov, A. A. Petrova, M. S. Fadeeva, F. E. Gostev, I. V. Shelaev, V. A. Nadtochenko and A. Yu. Semenov, *Biochemistry (Moscow)*, 2024, **89**, 1133; https://doi.org/10.1134/S0006297924060129.
S56 C. Consani, M. Prémont-Schwarz, A. ElNahhas, C. Bressler, F. van Mourik, A. Cannizzo and M. Chergui, *Angew. Chem., Int. Edit.*, 2009, **48**, 7184; https://doi.org/10.1002/anie.200902728.
S57 A. Mokhtari, J. Chesnoy and A. Laubereau, *Chem. Phys. Lett.*, 1989, **155**, 593; https://doi.org/10.1016/0009-2614(89)87479-2.
S58 G. Zgrablić, K. Voïtchovsky, M. Kindermann, S. Haacke, and M. Chergui, *Biophys. J.*, 2005, **88**, 2779; https://doi.org/10.1529/biophysj.104.046094.
S59 P. Hamm, M. Lim and R. M. Hochstrasser, *J. Phys. Chem. B*, 1998, **102**, 6123; https://doi.org/10.1021/jp9813286.

S60 V. Balzani and A. Juris, *Coord. Chem. Rev*., 2001, **211**, 97; https://doi.org/10.1016/S0010-8545(00)00274-5.
S61 R. Borrego-Varillas, D. C. Teles-Ferreira, A. Nenov, I. Conti, L. Ganzer, C. Manzoni, M. Garavelli, A. Maria de Paula and G. Cerullo, *J. Am. Chem. Soc.*, 2018, **140**, 16087; https://doi.org/10.1021/jacs.8b07057.
S62 G. Auböck, C. Consani, R. Monni, A. Cannizzo, F. van Mourik, and M. Chergui, *Rev. Sci. Instrum*., 2012, **83**, 093105; https://doi.org/10.1063/1.4750978.
S63 E. Baldini, T. Palmieri, E. Pomarico, G. Auböck and M. Chergui, *ACS Photonics*, 2018, **5**, 1241; https://doi.org/10.1021/acsphotonics.7b00945.
S64 P. Hamm, M. Lim, W. F. DeGrado, and R.M. Hochstrasser, *Proc. Natl. Acad. Sci. USA*, 1999, **96**, 2036; https://doi.org/10.1073/pnas.96.5.2036.
S65 B. Winter and M. Faubel, *Chem. Rev*., 2006, **106**, 1176; https://doi.org/10.1021/cr040381p.
S66 O. Link, E. Lugovoy, K. Siefermann, Y. Liu, M. Faubel and B. Abel, *Appl. Phys. A*, 2009, **96**, 117; https://doi.org/10.1007/s00339-009-5179-1.
S67 X. F. Li, A. L. Huillier, M. Ferray, L. A. Lompré and G. Mainfray, *Phys. Rev. A*, 1989, **39**, 5751; https://doi.org/10.1103/PhysRevA.39.5751.
S68 O. Link, E. Vöhringer-Martinez, E. Lugovoy, Y. Liu, K. Siefermann, M. Faubel, M. Grubmüller, R. B. Gerber, Y. Miller and B. Abel, *Faraday Discuss.*, 2009, **141**, 67; https://doi.org/10.1039/B811659H.
S69 J. Ojeda, C. A. Arrell, J. Grilj, F. Frassetto, L. Mewes, H. Zhang, F. van Mourik, L. Poletto and M. Chergui, *Struct. Dyn*., 2016, **3**, 023602; https://doi.org/10.1063/1.4933008.
S70 T. Elsaesser and M. Woerner, *Acta Crystallogr. A: Found. Crystallogr*., 2010, **66**, 168; https://doi.org/10.1107/S0108767309048181.
S71 R. W. Schoenlein, S. Chattopadhyay, H. H. W. Chong, T. E. Glover, P. A. Heimann, C. V. Shank, A. A. Zholents and M. S. Zolotorev, *Science*, 2000, **287**, 2237; https://doi.org/10.1126/science.287.5461.2237.
S72 M. Chergui, *Struct. Dyn*., 2016, **3**, 031001; https://doi.org/10.1063/1.4953104.
S73 E. M. Glebov, V. P. Grivin, D. B. Vasilchenko, A. V. Zadesenets and V. F. Plyusnin, *High Energy Chem*., 2017, **51**, 409; https://doi.org/10.1134/S0018143917060078.
S74 A. A. Shushakov, I. P. Pozdnyakov, V. P. Grivin, V. F. Plyusnin, D. B. Vasilchenko, A. V. Zadesenets, A. A. Melnikov, S. V. Chekalin and E. M. Glebov, *Dalton Trans.*, 2017, 46, 9440; https://doi.org/10.1039/C7DT01529A.
S75 V. V. Semionova, I. P. Pozdnyakov, V. P. Grivin, I. V. Eltsov, D. B. Vasilchenko, E. V. Polyakova, A. A. Melnikov, S. V. Chekalin, L. Wang and E. M. Glebov, *Photochem. Photobiol. Sci.*, 2024, **23**, 153; https://doi.org/10.1007/s43630-023-00509-y.